The *Caulerpa* Pigment Caulerpin Inhibits HIF-1 Activation and Mitochondrial Respiration

Yang Liu,[†] J. Brian Morgan,[†] Veena Coothankandaswamy,[†] Rui Liu,[†] Mika B. Jekabsons,[‡] Fakhri Mahdi,[†] Dale G. Nagle,*[,†,§] and Yu-Dong Zhou*[,†]

Department of Pharmacognosy and Research Institute of Pharmaceutical Sciences, School of Pharmacy, University of Mississippi, University, Mississippi 38677, and Department of Biology, University of Mississippi, University, Mississippi 38677

Received September 18, 2009

The transcription factor hypoxia-inducible factor-1 (HIF-1) represents an important molecular target for anticancer drug discovery. In a T47D cell-based reporter assay, the *Caulerpa* spp. algal pigment caulerpin (**1**) inhibited hypoxia-induced as well as 1,10-phenanthroline-induced HIF-1 activation. The angiogenic factor vascular endothelial growth factor (VEGF) is regulated by HIF-1. Caulerpin (10 μM) suppressed hypoxic induction of secreted VEGF protein and the ability of hypoxic T47D cell-conditioned media to promote tumor angiogenesis in vitro. Under hypoxic conditions, **1** (10 μM) blocked the induction of HIF-1α protein, the oxygen-regulated subunit that controls HIF-1 activity. Reactive oxygen species produced by mitochondrial complex III are believed to act as a signal of cellular hypoxia that leads to HIF-1α protein induction and activation. Further mechanistic studies revealed that **1** inhibits mitochondrial respiration at electron transport chain (ETC) complex I (NADH-ubiquinone oxidoreductase). Under hypoxic conditions, it is proposed that **1** may disrupt mitochondrial ROS-regulated HIF-1 activation and HIF-1 downstream target gene expression by inhibiting the transport or delivery of electrons to complex III.

The transcription factor HIF-1 (hypoxia-inducible factor-1) regulates oxygen homeostasis. First identified by Semenza and colleagues, HIF-1 is composed of the oxygen-regulated HIF-1α and the constitutively expressed HIF-1β/aryl hydrocarbon receptor nuclear translocator (ARNT) subunits.[1,2] Under normoxic conditions, HIF-1α protein is rapidly degraded and HIF-1 is inactive.[3] When the level of oxygen is reduced (hypoxia), the prolyl hydroxylases that modify HIF-1α protein and tag it for degradation are inhibited and HIF-1α protein is stabilized.[4−6] Hypoxia also inhibits the asparaginyl hydroxylase that modifies and inactivates HIF-1α protein.[7] As a result, hypoxia activates HIF-1 and its downstream targets. Both the prolyl and the asparaginyl hydroxylases that modify HIF-1α protein require ferrous iron (Fe^{2+}) as a cofactor.[4−7] Iron chelators (desferroxamine, 1,10-phenanthroline) and transition metals (Co^{2+}) inhibit these hydroxylases and activate HIF-1 under normoxic conditions. In addition to hypoxia and iron chelators, the activation of oncogenes (ras, src, myc, etc.) and/or the inactivation of tumor suppressor genes (i.e., PTEN, VHL) can also activate HIF-1.[8] In tumor cells, the activation of HIF-1 and the signaling pathways regulated by HIF-1 promotes adaptation and survival under hypoxic conditions that are commonly found in solid tumors.[8,9] Among cancer patients, the expression of HIF-1α protein correlates with advanced disease stages and resistance to treatments.[8,9] In animal-based studies, inhibition of HIF-1 suppressed tumor growth and enhanced treatment outcome when combined with radiation and chemotherapeutic agents.[10−16] Agents that inhibit HIF-1 (e.g., the HIF-1A RNA antagonist EZN-2968 and the small molecule PX-478, which decreases HIF-1A gene expression) are under early stage clinical evaluation for cancer treatment.[17] Numerous efforts are underway in industry, government, and academic laboratories to discover and develop small-molecule HIF-1 inhibitors for the treatment of cancer.

We have established a natural product chemistry-based program to discover small-molecule HIF-1 inhibitors. A human breast tumor T47D cell-based reporter assay was used to monitor the activity of HIF-1.[18] Natural product-rich extracts and pure compounds were examined in this 96-well plate formatted reporter assay for activities that inhibit hypoxia (1% O_2)-induced HIF-1 activation. The chlorophyte pigment caulerpin (**1**) suppressed HIF-1 activation. First isolated from the green algal genus *Caulerpa*,[19] **1** was found in certain species of *Caulerpa*[20] and in the red alga *Chondria armata*.[21] The effects of **1** on HIF-1 and its downstream targets were evaluated in human breast tumor cell-based systems. Compound **1** suppressed hypoxic activation of HIF-1 and the downstream targets examined. Mechanistic investigation revealed that **1** inhibited mitochondrial respiration at complex I.

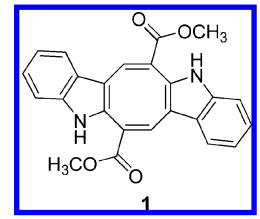

1

Results and Discussion

Concentration−response studies were performed to determine the effects of **1** on the activation of HIF-1 in a T47D cell-based reporter assay.[18] Compound **1** inhibited both hypoxia (1% O_2)- and chemical hypoxia (10 μM 1,10-phenanthroline)-induced HIF-1 activation with comparable potency (Figure 1A). Neither T47D cell viability nor luciferase expression from a pGL3-control construct (Promega) was affected by **1** at 30 μM (≤10% inhibition, hypoxic conditions, 16 h, data not shown). The effects of **1** on the induction of HIF-1 target genes vascular endothelial growth factor (VEGF) and glucose transporter-1 (GLUT-1) were examined in T47D cells. Both hypoxic exposure (1% O_2, 16 h) and treatment with an iron chelator (10 μM 1,10-phenanthroline, 16 h) increased the expression of VEGF and GLUT-1 at the mRNA level (*GLUT-1*, Figure 1B; *VEGF*, Figure 1C), relative to the untreated control. Compound **1** suppressed the induction of VEGF and GLUT-1 mRNAs by hypoxia at a concentration of 30 μM (0 versus 30 μM **1** under hypoxia, Figure 1B and C). No inhibition was observed when **1** was tested at a concentration of 10 μM (data not shown). The induction of VEGF and GLUT-1 mRNAs by 1,10-phenanthroline was not inhibited by **1** (Figure 1B and C).

The angiogenic factor VEGF plays an important role in tumor angiogenesis, and agents that inhibit VEGF are in clinical use for

* Joint corresponding authors. (D.G.N.) Tel: (662) 915-7026. Fax: (662) 915-6975. E-mail: dnagle@olemiss.edu. (Y.-D.Z.) Tel: (662) 915-7026. Fax: (662) 915-6975. E-mail: ydzhou@olemiss.edu.
[†] Department of Pharmacognosy.
[‡] Department of Biology.
[§] Research Institute of Pharmaceutical Sciences.

10.1021/np9005794
Published on Web 11/18/2009

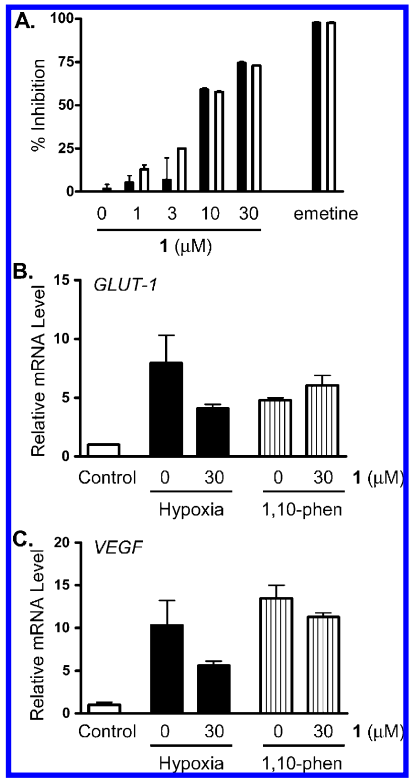

Figure 1. Caulerpin (**1**) inhibits HIF-1 activation. (A) Compound **1** inhibited hypoxia (1% O_2, 16 h, solid bar)- and 1,10-phenanthroline (10 μM, 16 h, open bar)-induced HIF-1 activation in a concentration-dependent manner in a T47D cell-based reporter assay. The positive control emetine was tested at 1 μM. Data shown are averages, and the bars represent standard deviation (representative one of two independent experiments in triplicate). (B) Compound **1** inhibited the induction of GLUT-1 mRNA by hypoxia (1% O_2, 16 h) in T47D cells. The levels of GLUT-1 mRNA were determined by quantitative real-time RT-PCR and normalized to an internal control (18S rRNA) using the $\Delta\Delta C_T$ method. The "Control" represents untreated cells. (C) Compound **1** inhibited hypoxic induction of VEGF mRNA. Data acquisition and processing were the same as those described in (B).

cancer.[22] One mechanism for hypoxia-stimulated tumor angiogenesis is by increased production of angiogenic factors (i.e., VEGF) by tumor cells.[22] The effect of **1** on hypoxic induction of VEGF protein was examined in T47D cells. The levels of VEGF proteins were determined by ELISA, and the data were normalized to the amount of cellular proteins (cellular VEGF protein, Figure 2A; secreted VEGF protein, Figure 2B). Compound **1** (10 μM) suppressed the induction of secreted VEGF protein by hypoxia. Since **1** did not affect the level of secreted VEGF protein under normoxic conditions, it is most likely that **1** suppressed hypoxic induction of secreted VEGF protein by reducing the level of VEGF protein under hypoxic conditions. Secreted VEGF protein constitutes $\geq$85% of total VEGF protein (0.37 pg of secreted VEGF protein versus 0.06 pg of cellular VEGF protein per μg of cellular protein, Figure 2A and B). To investigate if this decrease in the level of secreted VEGF protein translates into the suppression of tumor angiogenesis, a human umbilical vein endothelial cell (HUVEC)-based tube formation assay was employed as an in vitro model for tumor angiogenesis.[23] In the absence of stimuli, HUVEC cells were scattered (Basal Media, Figure 2C). Addition of recombinant human VEGF protein (VEGF, Figure 2C) as positive control or normoxic and hypoxic T47D cell-conditioned media induced HUVEC cells to form tube-like structures (Normoxic Control and Hypoxic Control, Figure 2C). An enhanced tube formation activity was observed with the conditioned media sample collected from hypoxic T47D cells, in comparison to that from normoxic T47D cells. Compound **1** suppressed the angiogenesis-inducing activity of hypoxic T47D cells [Hypoxia, **1** (10 μM) and Hypoxia, **1** (30 μM), Figure 2C). In contrast, **1** did not inhibit the angiogenic activity of normoxic T47D cell-conditioned media [**1** (30 μM), Figure 2C], suggesting that **1** does not interfere with the tube formation process. Two parameters often used to quantify the extent of angiogenesis in the tube formation assay are the length of tubes and the number of branching points. The inhibition of tumor angiogenesis by **1** correlates with the decreases in both the length of tubes (Figure 2D) and the number of branching points (Figure 2E). It is most likely that **1** suppresses tumor angiogenesis by blocking the hypoxic induction of angiogenic factors such as VEGF. The observation that **1** (10 μM) exerted a more pronounced effect on secreted VEGF level, in comparison to that at the mRNA level, suggests that **1** may also exert HIF-1-independent post-transcriptional effects.

Hypoxia-stimulated tumor cell invasion and metastasis represent a significant contributor to the malignant progression of tumors, and HIF-1 regulates the expression of a number of genes that are involved in the complex metastatic process.[24] To assess the effect of **1** on tumor cell migration, a metastatic MDA-MB-231 human breast tumor cell-based wound-healing assay was used as an in vitro model. A "wound" was created by scratching a layer of confluent MDA-MB-231 cells with a 200 μL pipet tip. Surrounding cells migrate into the damaged area, resulting in the healing of the "wound" over a period of time (22 h). Compound **1** suppressed the migration of MDA-MB-231 cells in a concentration-dependent manner (Figure 3A). To exclude the possibility that the inhibition of migration was due to cytotoxicity, the effect of **1** on the proliferation/viability of MDA-MB-231 cells was examined using the neutral red method. Under experimental conditions (22 h, normoxia and hypoxia), **1** did not exert a significant effect on the viability of MDA-MB-231 cells (less than 15% inhibition, Figure 3B).

The effects of **1** on cell growth/viability were further examined in a panel of human tumor cell lines (breast tumor T47D, MCF-7, and MDA-MB-231; prostate tumor DU145 and PC-3) and primary human mammary epithelial cells (HMEC, Lonza), which were used as an in vitro model for normal cells. A cell line-dependent growth inhibitory effect was observed in this 48 h exposure study (Figure 4). Extended incubation time (48 h versus 22 h) led to an increase in growth inhibition in MDA-MB-231 cells (Figure 3B versus Figure 4). The highest level of inhibition was 52% in PC-3 cells at a concentration of 30 μM. The normal HMEC cells were affected to a lesser extent (less than 25% at concentrations up to 30 μM). DU145 cells were least sensitive to **1**.

To investigate the mechanism of action for **1** to inhibit HIF-1 activation, the effect of **1** on the induction of HIF-1α protein was evaluated by Western blot. In general, the induction of HIF-1α protein correlates with the activation of HIF-1. Hypoxic exposure (1% O_2, 4 h) and 1,10-phenanthroline treatment (10 μM, 4 h) each induced the accumulation of HIF-1α protein in the nuclear extract samples prepared from T47D cells (Figure 5A). At the concentration of 10 μM, **1** blocked the induction of HIF-1α protein by hypoxia (Figure 5A). The inhibitory effect was less pronounced on 1,10-phenanthroline (chemical hypoxia)-induced accumulation of nuclear HIF-1α protein (Figure 5A). Levels of the constitutively expressed HIF-1β protein in the nuclear extract samples were monitored by Western blot as a control (Figure 5A). Compound **1** did not decrease the levels of HIF-1β protein. Among the small-molecule HIF-1 inhibitors that we and others have examined, compounds that disrupt the function of mitochondria selectively inhibited HIF-1 activation by hypoxia, relative to that by other stimuli (iron chelators, anoxia, etc.).[18,25,26] A T47D cell-based respiration study was performed to determine the effect of **1** on cellular oxygen consumption.[26] In nonpermeabilized T47D cells, **1** reduced the rate of cellular

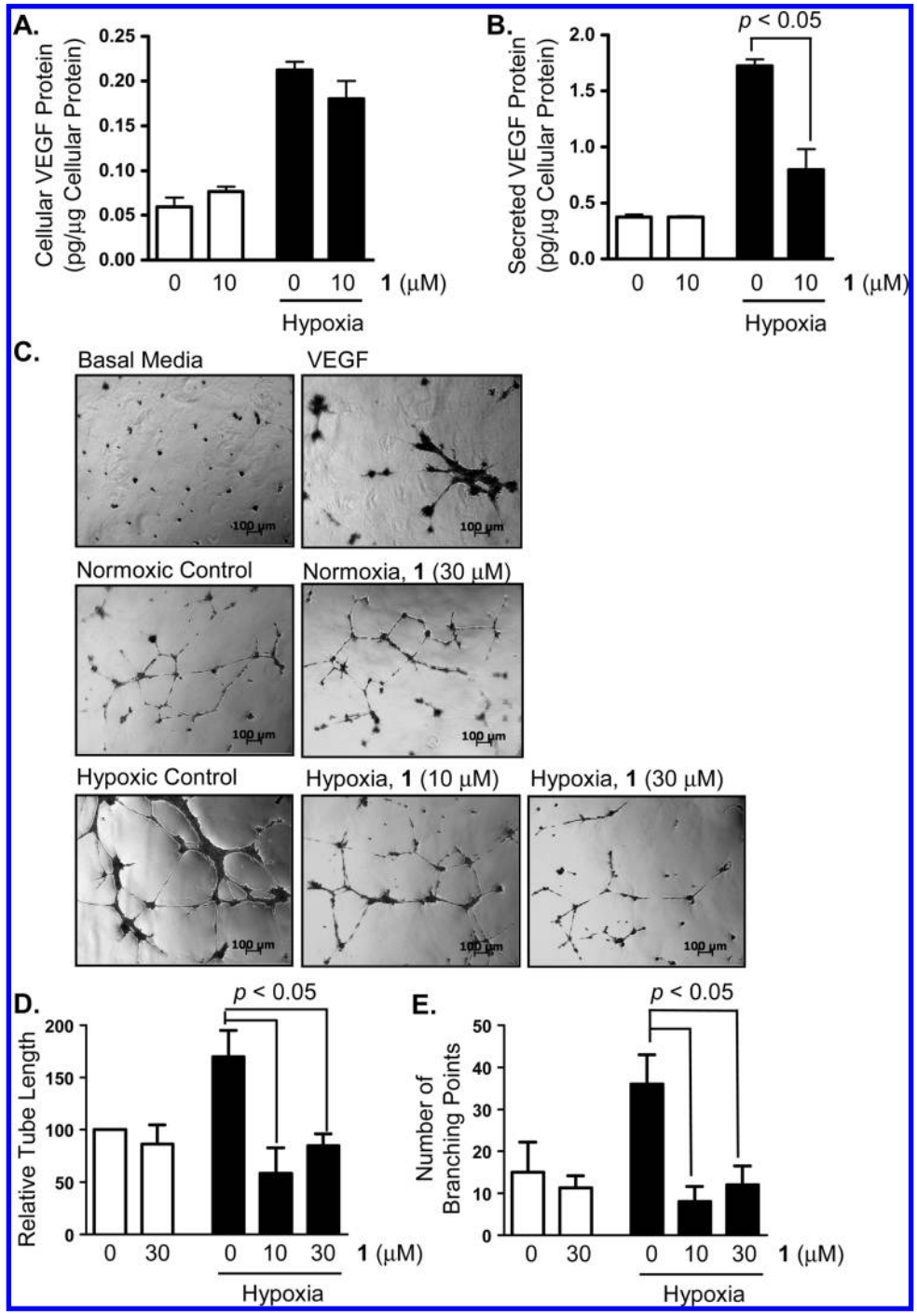

Figure 2. Caulerpin (**1**) inhibits hypoxic induction of secreted VEGF protein and tumor angiogenesis in vitro. (A) Levels of cellular VEGF protein in the lysates of T47D cells exposed to hypoxia (1% O_2, 16 h, solid bar) in the presence of **1** were determined by ELISA and normalized to the amounts of cellular proteins (average + standard deviation, representative one of two independent experiments in triplicate). Data acquired under normoxic conditions (5% CO_2/95% air, 16 h) are shown with open bars. (B) Levels of secreted VEGF protein in the media conditioned by T47D cells exposed to hypoxia (1% O_2, 16 h) in the presence of **1**. Data acquisition and presentation are the same as those described in (A). The *p* value is provided when there is a statistically significant difference between the induced and the compound-treated samples. (C) The effects of **1** on tumor angiogenesis were evaluated in a HUVEC tube formation assay with T47D cell-conditioned media samples. Representative image of each condition is shown with a 100 μm scale bar. The positive (VEGF) and negative (Basal Media) controls are included at the top. The extent of tube formation induced by T47D cell-conditioned media samples (Figure 2C) was quantified in three randomly selected fields for each condition. The data [tube length (D); and number of branching point (E)] are averages, and the bars represent standard deviation.

respiration in a concentration-dependent manner (no effect at 10 μM and 30% inhibition at 30 μM, data from preliminary studies not shown). Preincubation of T47D cells with **1** at 37 °C for 2 h dramatically reduced cellular respiration rate (87% reduction in T47D cells treated with 30 μM **1**, relative to the untreated control, data from preliminary studies not shown). Permeabilization of the plasma membrane with digitonin significantly enhanced the inhibitory effect exerted by **1** on mitochondrial respiration (57% inhibition at 30 μM, Figure 5B). Thus, it is likely that **1** does not penetrate cells readily and extended incubation facilitates compound uptake. To discern the component(s) of the mitochondrial electron transport chain (ETC) affected by **1**, further mechanistic studies were

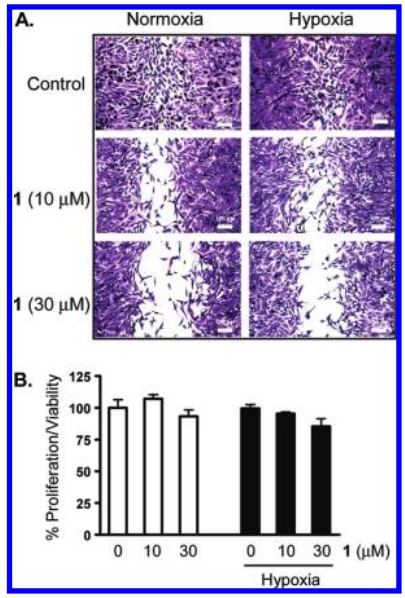

Figure 3. Caulerpin (**1**) inhibits the migration of MDA-MB-231 cells. (A) The effect of **1** on tumor cell migration was examined in a MDA-MB-231 cell-based wound-healing assay. Wounds (600 μm width) were created by scratching a layer of confluent MDA-MB-231 cells with 200 μL pipet tips. The incubation continued for 22 h in DMEM/F12 media supplemented with 5% FBS in the presence and absence of **1**, under normoxic and hypoxic conditions. The cells were fixed in methanol and stained with crystal violet. Scale bars (100 μm) are included inside each picture. (B) The effect of **1** on the proliferation/viability of MDA-MB-231 cells under the conditions used in the wound-healing assay was determined by the neutral red method. Data are presented as % control of the untreated cells (average + standard deviation, one experiment in triplicate).

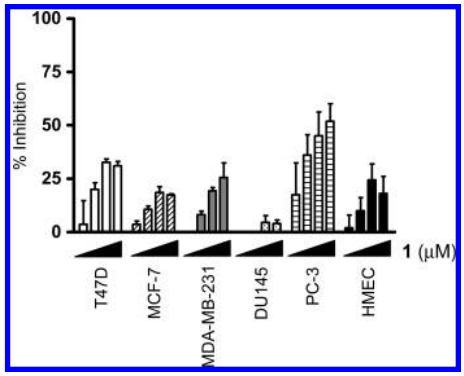

Figure 4. Caulerpin (**1**) exerts cell line-dependent growth inhibitory effects. Exponentially grown cells were plated into 96-well plates and exposed to **1** at concentrations of 1, 3, 10, and 30 μM for 48 h under normoxic conditions, and cell viability was determined by the sulforhodamine B method. Data (average + standard deviation, one experiment in triplicate) are presented as % inhibition calculated using the following formula: % inhibition = $(1 - OD_{treated}/OD_{control}) \times 100$.

performed. The first study examined the function of the mitochondrial ETC in cells treated with **1**. The extent of mitochondrial respiration correlates with the rate of oxygen consumption, determined using an Oxytherm Clarke-type electrode system (Hansatech). The T47D cells treated with **1** (30 μM, 37 °C, 2 h) were trypsinized and resuspended in a buffer solution, and the plasma membrane was permeabilized with digitonin. Addition of a mixture of malate and pyruvate (ETC complex I substrates) failed to initiate mitochondrial respiration in T47D cells pretreated with **1** (Figure 5C), relative to their ability to initiate respiration in control

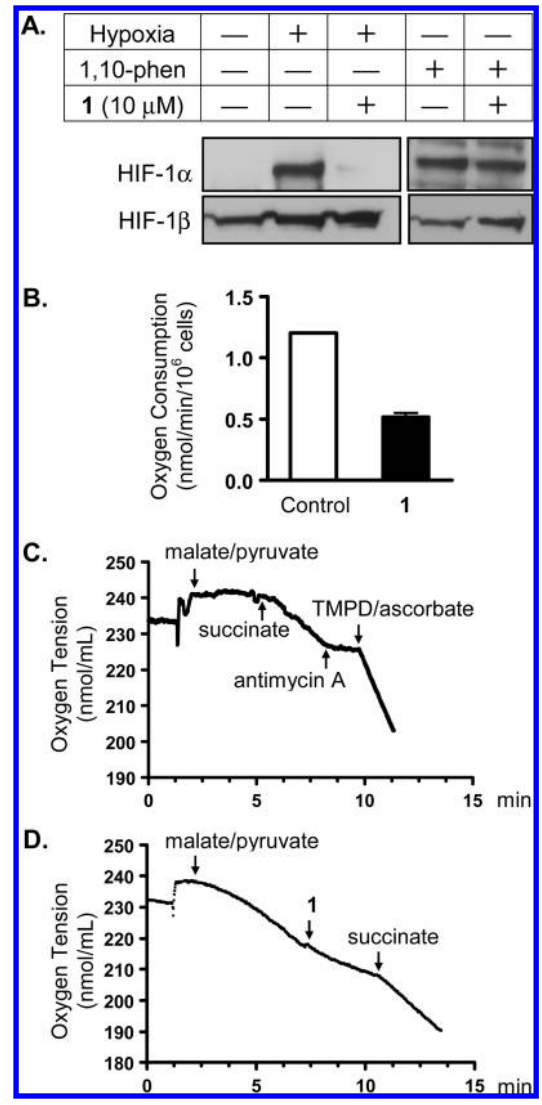

Figure 5. Caulerpin (**1**) blocks hypoxic induction of HIF-1α protein and suppresses mitochondrial respiration at complex I. (A) Levels of HIF-1α and HIF-1β proteins in nuclear extract samples prepared from T47D cells exposed to hypoxia (1% O_2, 4 h) or 1,10-phenanthroline (10 μM) in the presence and absence of **1** were determined by western blot analysis. (B) Compound **1** (30 μM) inhibited mitochondrial oxygen consumption in T47D cells permeabilized with digitonin (30 μM). Data shown are averages from three determinations, and the bars indicate standard deviation. (C) The ETC complex I was suppressed in compound **1**-treated T47D cells, while complexes II, III, and IV remained functional. The T47D cells were treated with **1** (30 μM) at 37 °C for 2 h. The cells were trypsinized, washed, and resuspended in a buffer solution. Substrates and inhibitors were added in a sequential manner to T47D cells (5×10^6, 30 °C) at the specified time point. (D) Compound **1** (30 μM) inhibits mitochondria respiration by targeting complex I in T47D cells.

cells.[25,26] Succinate (complex II substrate) initiated mitochondrial respiration in these T47D cells that were previously treated with **1**. These observations indicate that **1** treatment impaired complex I. To ensure that the ETC remained functional, antimycin A (complex III inhibitor) was added to suppress respiration in the presence of succinate, and a mixture of TMPD/ascorbate (complex IV substrates) was added to reinitiate respiration (Figure 5C). These results suggest that compound **1** inhibited ETC complex I without affecting complexes II, III, and IV. For confirmation, compound **1** (30 μM) was added to permeabilized T47D cells respiring in the presence of malate and pyruvate (Figure 5D). Compound **1**

suppressed mitochondrial respiration, and the inhibition was relieved by the complex II substrate succinate (Figure 5D), just as observed with other ETC complex I inhibitors (e.g., rotenone).[27,28]

Mitochondrial mediated reactive oxygen species (ROS) signaling leads to the stabilization of HIF-1α protein and the subsequent activation of HIF-1.[27−29] Hypoxia suppresses the transfer of electron to oxygen at mitochondrial ETC complex IV and increases ROS generation at complexes I and III. Complex I inhibitors such as rotenone and diphenylene iodonium (DPI) curb complex III superoxide anion ROS production and destabilize HIF-1α protein under hypoxic conditions.[29] It is likely that **1** blocks the hypoxic induction of HIF-1α protein by inhibiting complex III superoxide anion generation, as previously observed with other complex I inhibitors.

Caulerpin was first isolated from green algae of the genus *Caulerpa* as a red pigment.[19] A survey of caulerpin distribution in species of the genus *Caulerpa* revealed that the presence of caulerpin correlates with the bilateral morphology and the absence of peroxidase activity.[20,30] Caulerpin was subsequently isolated from the red alga *Chondria armata*.[21] Cardellina and colleagues hypothesized that caulerpin may regulate plant growth and demonstrated that caulerpin functions as an auxin in a lettuce seedling root growth assay.[30] Other reported bioactivities of caulerpin include (1) the inhibition of human protein tyrosine phosphatase 1B (hPTP1B)[31] and (2) the ability to restore the growth of a yeast strain that overexpresses the human indoleamine 2,3-dioxygenase (IDO) gene.[32] In male Swiss mice, caulerpin exhibited no acute toxicity when administered at the maximum dose of 2 g kg^{-1} orally or at 0.2 g kg^{-1} intravenously.[33] However, caulerpin has recently been shown to be cytotoxic to human dermal fibroblasts (FEK4).[34] Our study is the first characterization of caulerpin as a cellular hypoxia-targeted antitumor agent. The observations that caulerpin suppresses HIF-1 activation and downstream HIF pathways (i.e., tumor angiogenesis) support further exploration of the anticancer potential of caulerpin.

The finding that caulerpin suppresses mitochondrial respiration at complex I may shed light on why the green algae *Caulerpa taxifolia* can survive and invade the waters of the Mediterranean. Dubbed the "killer algae", an aquarium-bred strain of *C. taxifolia* was originally dumped into the Mediterranean in 1984. This alga has been devastating coastal ecosystems by invading over 10 000 acres of the Mediterranean coast over a period of two decades.[35] It was reported that caulerpin constitutes 0.05% dry weight of a Chinese *C. taxifolia* sample.[31] The mitochondrial complex I inhibitor rotenone and the roots of plants belonging to the genus *Loncocarpus* that contain rotenone have been used as fish poisons for centuries.[36] The purified compound rotenone is a potent toxin to fish and snails, and it is used commercially as a piscicide and agricultural pesticide. It is a logical extension to speculate that fishes and other marine animals will avoid eating algae that contain inhibitors of mitochondrial respiration. While studies have not shown a direct effect of caulerpin on herbivore grazing,[37,38] it remains likely that the mitochondrial inhibitor caulerpin plays some form of protective role in the *C. taxifolia* chemical ecology. Caulerpin has been shown to increase the susceptibility of marine invertebrates to environmental toxins by inhibiting the P-glycoprotein transporter that produces multixenobiotic resistance (MXR).[39] Therefore, caulerpin may also potentiate the toxic effects of other *Caulerpa* metabolites to fish and marine invertebrates by blocking MXR-mediated efflux. The MXR P-glycoprotein transporter is an ATP-dependent plasma membrane efflux pump. As in the case of rotenone, the ability of caulerpin to inhibit MXR may be explained by the effect of caulerpin on the mitochondrial electron transport chain and ATP production.[40] In addition, the plant growth regulatory function of caulerpin may promote the expansion of *C. taxifolia*. As a result, the combined force of self-promoted growth and chemical defenses may contribute to the invasive nature of the "killer algae".

Experimental Section

Caulerpin (1). The sample was from the University of Mississippi purified natural product repository. The structure and purity of the sample were confirmed by NMR analysis. Orange crystals; ESIMS *m/z* 399 $[M + H]^+$, molecular formula $C_{24}H_{18}N_2O_4$. The 400 MHz ^1H and 100 MHz ^{13}C NMR spectra recorded in DMSO-d_6 on AMX-NMR spectrometers (Bruker) matched those previously published.[34,41]

Cell-Based Reporter Assay. The T47D cell-based reporter assay for HIF-1 activity was the same as previously described.[18,26] Compound **1** was dissolved in DMSO and the stock solution (4 mM) stored at −20 °C. Final solvent concentration was less than 0.25% (v/v). The data were presented as % inhibition of the induced sample using the formula

$$\% \text{ inhibition} = (1 - \text{light output}_{\text{treated}}/\text{light output}_{\text{induced}}) \times 100$$

Real-Time RT-PCR. The acquisition of total RNA samples from compound-treated and control T47D cells, cDNA synthesis, sequences of the gene-specific primers, real-time PCR reaction, data analysis, and presentation were the same as those described.[42]

ELISA Assay for VEGF Protein and HUVEC-Based Tube Formation. The procedures were previously described in detail.[18,26] The ELISA data were presented as levels of VEGF proteins normalized to the quantity of cellular proteins. The HUVEC-based tube formation assay was performed and analyzed as described.[26]

MDA-MB-231 Cell-Based Wound-Healing Assay. MDA-MB-231 cells (ATCC) were maintained in DMEM/F12 media with L-glutamine (Mediatech), supplemented with 10% (v/v) fetal bovine serum (FBS, Hyclone), 50 units/mL penicillin, and 50 μg mL^{-1} streptomycin (BioWhittaker). A detailed procedure for the wound-healing assay was described.[25,26]

Cell Proliferation/Viability Assay. Human T47D, MCF-7, MDA-MB-231, DU-145, and PC-3 cell lines were purchased from ATCC and maintained in DMEM/F12 media supplemented with 10% FBS (Hyclone), 50 units mL^{-1} penicillin, and 50 μg mL^{-1} streptomycin (Biowhittaker). Human mammary epithelial cells (HMEC) were acquired from Lonza and maintained as instructed by the supplier. Exponentially grown cells were plated at a density of 30 000 cells per well in a volume of 100 μL of culture media supplemented with FBS and antibiotics into 96-well plates (Greiner Bio-One). After the cells attach (overnight), test compounds were diluted with serum-free media and added to the specified wells in a volume of 100 μL. The incubation continued for 48 h under normoxic conditions (95% air/5% CO_2, 37 °C), and cell viability was determined using the sulforhodamine B method.[26,43] Light absorbance at 490 nm was determined on a BioTek Synergy plate reader with background absorbance at 690 nm. A formula similar to the one described in the reporter section was applied to calculate the % inhibition data.

Nuclear Extract Preparation and Western Blot Analysis. T47D cells (10×10^6 cells per 100 mm plate) were exposed to test compounds or media for 30 min, and the incubation continued for another 4 h under hypoxic conditions (1% O_2/5% CO_2/94% N_2) or in the presence of 1,10-phenanthroline (10 μM). The preparation of nuclear extract samples from T47D cells and the determination of the levels of HIF-1α and HIF-1β proteins in the nuclear extract samples by Western blot were the same as those described in detail.[18,26]

Mitochondrial Respiration Assays. A method used to monitor respiration in isolated mitochondria[44] was modified to measure the level of oxygen consumption in T47D cells and to investigate the specific target within the mitochondrial electron transport chain affected by active compounds.[25,26] For the incubation study, T47D cells were seeded at a density of 5×10^6 cells per 100 mm plate. After overnight incubation, half of the conditioned media were replaced with serum-free media that contain test compound and the incubation continued for another 2 h. The cells were trypsinized, collected, and permeabilized, and the respiration studies performed as described.[25,26] The mechanistic study to discern the site within the mitochondrial ETC regulated by the active compound was performed as previously described.[25,26]

Statistical Analysis. Data were compared using one-way ANOVA and Bonfferoni post hoc analyses (GraphPad Prism 4). Differences were considered significant when $p < 0.05$.

Acknowledgment. The authors thank Dr. S. L. McKnight at the University of Texas Southwestern Medical Center at Dallas for providing the pTK-HRE3-luc construct. Funding was provided in part by the NIH/NCI grant CA98787 (D.G.N./Y.D.Z.), NOAA/NIUST grant NA16RU1496, and NIH/NCRR grant P20RR021929. This investigation was conducted in a facility constructed with Research Facilities Improvement Grant C06 RR-14503-01 from the NIH.

Supporting Information Available: Spectroscopic data (^{1}H and ^{13}C NMR spectra) for **1**. This material is available free of charge via the Internet at http://pubs.acs.org.

References and Notes

(1) Semenza, G. L.; Wang, G. L. *Mol. Cell. Biol.* **1992**, *12*, 5447–5454.
(2) Wang, G. L.; Semenza, G. L. *J. Biol. Chem.* **1995**, *270*, 1230–1237.
(3) Maxwell, P. H.; Wiesener, M. S.; Chang, G. W.; Clifford, S. C.; Vaux, E. C.; Cockman, M. E.; Wykoff, C. C.; Pugh, C. W.; Maher, E. R.; Ratcliffe, P. J. *Nature* **1999**, *399*, 271–275.
(4) Ivan, M.; Kondo, K.; Yang, H.; Kim, W.; Valiando, J.; Ohh, M.; Salic, A.; Asara, J. M.; Lane, W. S.; Kaelin, W. G., Jr. *Science* **2001**, *292*, 464–468.
(5) Jaakkola, P.; Mole, D. R.; Tian, Y. M.; Wilson, M. I.; Gielbert, J.; Gaskell, S. J.; Kriegsheim, A.; Hebestreit, H. F.; Mukherji, M.; Schofield, C. J.; Maxwell, P. H.; Pugh, C. W.; Ratcliffe, P. J. *Science* **2001**, *292*, 468–472.
(6) Bruick, R. K.; McKnight, S. L. *Science* **2001**, *294*, 1337–1340.
(7) Lando, D.; Peet, D. J.; Whelan, D. A.; Gorman, J. J.; Whitelaw, M. L. *Science* **2002**, *295*, 858–861.
(8) Semenza, G. L. *Nat. Rev. Cancer* **2003**, *3*, 721–732.
(9) Tatum, J. L.; Kelloff, G. J.; Gillies, R. J.; Arbeit, J. M.; Brown, J. M.; Chao, K. S.; Chapman, J. D.; Eckelman, W. C.; Fyles, A. W.; Giaccia, A. J.; Hill, R. P.; Koch, C. J.; Krishna, M. C.; Krohn, K. A.; Lewis, J. S.; Mason, R. P.; Melillo, G.; Padhani, A. R.; Powis, G.; Rajendran, J. G.; Reba, R.; Robinson, S. P.; Semenza, G. L.; Swartz, H. M.; Vaupel, P.; Yang, D.; Croft, B.; Hoffman, J.; Liu, G.; Stone, H.; Sullivan, D. *Int. J. Radiat. Biol.* **2006**, *82*, 699–757.
(10) Ryan, H. E.; Poloni, M.; McNulty, W.; Elson, D.; Gassmann, M.; Arbeit, J. M.; Johnson, R. S. *Cancer Res.* **2000**, *60*, 4010–4015.
(11) Rapisarda, A.; Zalek, J.; Hollingshead, M.; Braunschweig, T.; Uranchimeg, B.; Bonomi, C. A.; Borgel, S. D.; Carter, J. P.; Hewitt, S. M.; Shoemaker, R. H.; Melillo, G. *Cancer Res.* **2004**, *64*, 6845–6848.
(12) Greenberger, L. M.; Horak, I. D.; Filpula, D.; Sapra, P.; Westergaard, M.; Frydenlund, H. F.; Albaek, C.; Schroder, H.; Orum, H. *Mol. Cancer Ther.* **2008**, *7*, 3598–3608.
(13) Unruh, A.; Ressel, A.; Mohamed, H. G.; Johnson, R. S.; Nadrowitz, R.; Richter, E.; Katschinski, D. M.; Wenger, R. H. *Oncogene* **2003**, *22*, 3213–3220.
(14) Moeller, B. J.; Dreher, M. R.; Rabbani, Z. N.; Schroeder, T.; Cao, Y.; Li, C. Y.; Dewhirst, M. W. *Cancer Cell* **2005**, *8*, 99–110.
(15) Li, L.; Lin, X.; Shoemaker, A. R.; Albert, D. H.; Fesik, S. W.; Shen, Y. *Clin. Cancer Res.* **2006**, *12*, 4747–4754.
(16) Cairns, R. A.; Papandreou, I.; Sutphin, P. D.; Denko, N. C. *Proc. Natl. Acad. Sci. U.S.A.* **2007**, *104*, 9445–9450.
(17) U.S. NIH database Clinical Trials.gov, http://www.clinicaltrials.gov/ct2/search, accessed July 22, 2009.
(18) Hodges, T. W.; Hossain, C. F.; Kim, Y. P.; Zhou, Y. D.; Nagle, D. G. *J. Nat. Prod.* **2004**, *67*, 767–771.
(19) Aguilar-Santos, G. *J. Chem. Soc., Perkin Trans. 1* **1970**, *6*, 842–843.
(20) Schwede, J. G.; Cardellina, J. H., II; Grode, S. H.; James, T. R., Jr.; Blackman, A. J. *Phytochemistry* **1987**, *26*, 155–158.
(21) Govenkar, M. B.; Wahidulla, S. *Phytochemistry* **2000**, *54*, 979–981.
(22) Ferrara, N.; Mass, R. D.; Campa, C.; Kim, R. *Annu. Rev. Med.* **2007**, *58*, 491–504.
(23) Helmlinger, G.; Endo, M.; Ferrara, N.; Hlatky, L.; Jain, R. K. *Nature* **2000**, *405*, 139–141.
(24) Liao, D.; Corle, C.; Seagroves, T. N.; Johnson, R. S. *Cancer Res.* **2007**, *67*, 563–572.
(25) Liu, Y.; Liu, R.; Mao, S. C.; Morgan, J. B.; Jekabsons, M. B.; Zhou, Y. D.; Nagle, D. G. *J. Nat. Prod.* **2008**, *71*, 1854–1860.
(26) Liu, Y.; Veena, C. K.; Morgan, J. B.; Mohammed, K. A.; Jekabsons, M. B.; Nagle, D. G.; Zhou, Y. D. *J. Biol. Chem.* **2009**, *284*, 5859–68.
(27) Guzy, R. D.; Hoyos, B.; Robin, E.; Chen, H.; Liu, L.; Mansfield, K. D.; Simon, M. C.; Hammerling, U.; Schumacker, P. T. *Cell Metab.* **2005**, *1*, 401–408.
(28) Simon, M. C. *Adv. Exp. Med. Biol.* **2006**, *588*, 165–170.
(29) Xia, C.; Meng, Q.; Liu, L. Z.; Rojanasakul, Y.; Wang, X. R.; Jiang, B. H. *Cancer Res.* **2007**, *67*, 10823–10830.
(30) Raub, M. F.; Cardellina, J. H., II; Schwede, J. G. *Phytochemistry* **1987**, *26*, 619–620.
(31) Mao, S. C.; Guo, Y. W.; Shen, X. *Bioorg. Med. Chem. Lett.* **2006**, *16*, 2947–2950.
(32) Vottero, E.; Balgi, A.; Woods, K.; Tugendreich, S.; Melese, T.; Andersen, R. J.; Mauk, A. G.; Roberge, M. *Biotechnol. J.* **2006**, *1*, 282–288.
(33) Vidal, J. P.; Laurent, D.; Kabore, S. A.; Rechencq, E.; Boucard, M.; Girard, J. P.; Escale, R.; Rossi, J. C. *Bot. Mar.* **1984**, *27*, 533–537.
(34) Rocha, F. D.; Soares, A. R.; Houghton, P. J.; Pereira, R. C.; Kaplan, M. A. C.; Teixeira, V. L. *Phytother. Res.* **2007**, *21*, 170–175.
(35) Meinesz, A. *Killer Algae*; University of Chicago Press: Chicago, 1999; p 360.
(36) Hocking, G. M. *A Dictionary of Natural Products*; Plexus Publishing, Inc.: Medford, 1997; pp 455−677.
(37) Paul, V. J.; Fenical, W. *Tetrahedron Lett.* **1982**, *23*, 5017–5020.
(38) Paul, V. J.; Littler, M. M.; Littler, D. S.; Fenical, W. *J. Chem. Ecol.* **1987**, *13*, 1171–1185.
(39) Schrõder, H. C.; Badria, F. A.; Ayyad, S. N.; Batel, R.; Wiens, M.; Hassanein, H. M. A.; Kurelec, B.; Mĺler, W. E. G. *Environ. Toxicol. Pharmacol.* **1998**, *5*, 119–126.
(40) Gyémánt, N.; Tanaka, M.; Antus, S.; Hohmann, J.; Csuka, O.; Mándoky, L.; Molnár, J. *In Vivo* **2005**, *19*, 367–374.
(41) Anjaneyulu, A. S. R.; Prakash, C. V. S.; Mallavadhani, U. V. *Phytochemistry* **1991**, *30*, 3041–3042.
(42) Hossain, C. F.; Kim, Y. P.; Baerson, S. R.; Zhang, L.; Bruick, R. K.; Mohammed, K. A.; Agarwal, A. K.; Nagle, D. G.; Zhou, Y. D. *Biochem. Biophys. Res. Commun.* **2005**, *333*, 1026–1033.
(43) Skehan, P.; Storeng, R.; Scudiero, D.; Monks, A.; McMahon, J.; Vistica, D.; Warren, J. T.; Bokesch, H.; Kenney, S.; Boyd, M. R. *J. Natl. Cancer Inst.* **1990**, *82*, 1107–1112.
(44) St-Pierre, J.; Buckingham, J. A.; Roebuck, S. J.; Brand, M. D. *J. Biol. Chem.* **2002**, *277*, 44784–44790.

NP9005794